Cassini plasma observations of Saturn's magnetospheric cusp

Jamie M. Jasinski[1,2,3], Christopher S. Arridge[4], Andrew J. Coates[1,3], Geraint H. Jones[1,3], Nick Sergis[5], Michelle F. Thomsen[6], Daniel B. Reisenfeld[7], Norbert Krupp[8], and J. Hunter Waite Jr.[9]

[1]Mullard Space Science Laboratory, UCL, London, UK, [2]Department of Climate and Space Sciences and Engineering, University of Michigan, Ann Arbor, Michigan, USA, [3]Centre for Planetary Sciences, UCL/Birkbeck, London, UK, [4]Department of Physics, Lancaster University, Lancaster, UK, [5]Office for Space Research and Technology, Academy of Athens, Athens, Greece, [6]Planetary Science Institute, Tucson, Arizona, USA, [7]Department of Physics and Astronomy, University of Montana, Missoula, Montana, USA, [8]Max-Planck-Institut für Sonnensystemforschung, Göttingen, Germany, [9]Southwest Research Institute, San Antonio, Texas, USA

Abstract The magnetospheric cusp is a funnel-shaped region where shocked solar wind plasma is able to enter the high-latitude magnetosphere via the process of magnetic reconnection. The plasma observations include various cusp signatures such as ion energy dispersions and diamagnetic effects. We present an overview analysis of cusp plasma observations at the Saturnian magnetosphere from the Cassini spacecraft era. A comparison of the observations is made as well as classification into groups due to varying characteristics. The locations of the reconnection site are calculated and shown to vary along the subsolar magnetopause. We show the first in situ evidence for lobe reconnection that occurred at nearly the same time as dayside reconnection for one of the cusp crossings. Evidence for "bursty" and more "continuous" reconnection signatures is observed at different cusp events. The events are compared to solar wind propagation models, and it is shown that magnetic reconnection and plasma injection into the cusp can occur for a variety of upstream conditions. These are important results because they show that Saturn's magnetospheric interaction with the solar wind and the resulting cusp signatures are dynamic and that plasma injection in the cusp occurs due to a variety of solar wind conditions. Furthermore, reconnection can proceed at a variety of locations along the magnetopause.

1. Introduction

Chapman and Ferraro [1931a, 1931b] were the first to postulate the idea of the magnetospheric cusp, showing that within the magnetosphere there would be a pair of magnetic "null" points, one in the northern hemisphere and one in the southern hemisphere. This magnetic funnel-shaped region of the cusp is always present due to the geometry of the field lines in an open magnetosphere. However, the direct entry of solar wind plasma into this region occurs via the process of magnetic reconnection between the interplanetary magnetic field (IMF) and closed magnetospheric field lines at the subsolar point, as well as the subsequent pole-ward convection of the open field line which is now known to be part of the Dungey Cycle [*Dungey*, 1961]. Consequently, the observation of open cusp field lines is usually identified through (injected solar wind) plasma in the high-latitude dayside magnetosphere from the reconnection site [e.g., *Frank*, 1971; *Russell et al.*, 1971; *Gosling et al.*, 1990]. Reconnection can also occur in the lobe region between the IMF and open magnetospheric field lines, which results in the newly reconnected field line convecting equatorward. Therefore, the cusps are important to study as they are a source of direct entry of matter, energy, and momentum into a magnetosphere. They are also well situated in space so as to observe and study the effects of reconnection, as the cusps map to a wide range of locations at the magnetopause. Much of the research which has been carried out on the topic of the cusp has been done for Earth [e.g., *Smith and Lockwood*, 1996 and *Cargill et al.*, 2005].

The observations in the cusp are of magnetosheath plasma, ions with low energies of a few hundred eV up to ~1 keV at Earth [e.g., *Heikkila and Winningham*, 1971; *Pitout et al.*, 2009]. The most characteristic cusp signature is that of the ion plasma displaying an energy-latitude (energy-time) dispersion. The particles that are injected have different energies (and therefore differing field-aligned velocities). This means that particles with two different energies will have a different time of flight along a field line. As a result, the particle with the higher

energy will travel faster along the field line. While the particles travel along the magnetic field, the flux tube is convecting poleward, causing the higher-energy particle to reach any point along the field line at a lower latitude than a lower energy particle. This results in lower energy particles reaching higher latitudes later (in time) along the field line than the higher-energy particles. Therefore, the particles become dispersed in latitude. This gives rise to the "velocity filter effect" [*Shelley et al.*, 1976; *Hill and Reiff*, 1977; *Reiff et al.*, 1977; *Lockwood et al.*, 1994] that is observed by a particle detector. A spacecraft that is moving through the cusp will observe an energy-latitude dispersion in the ions, whereby the higher-energy ions are observed at lower latitudes for a particular injection point.

After reconnection happens, the solar wind enters the magnetosphere along the open field line at the magnetopause. A spacecraft will observe plasma that has been injected from different areas along the magnetopause after reconnection. However, the lowest energy observed will be from the plasma that was injected first (at the reconnection site). Therefore, the low-energy ion cutoff represents the plasma injected from the reconnection site, and the higher energies simultaneously observed will be due to ions injected later in time that have "caught up" with the ion with the lowest energy. This is why the ion dispersions are marked by the lowest-energy ion cutoff.

Subsolar magnetopause reconnection occurs most favorably when the magnetosheath magnetic field is antiparallel to the magnetospheric field [*Burton et al.*, 1975; *Mozer and Retinò*, 2007]. At Saturn, subsolar magnetopause reconnection is therefore favored for northward IMF, while southward IMF favors a location antisunward of the cusp in the lobes, either in one hemisphere or in both [e.g., *Gosling et al.*, 1991; *Øieroset et al.*, 1997]. Due to magnetic tension forces, the reconnected magnetic field line at the lobes convects equatorward and so the ion energy-latitude dispersion observed is opposite to that discussed previously, with the higher-energy ions now observed at higher latitudes. This is called a "reverse-sense" dispersion (as opposed to a "normal-sense" dispersion for subsolar reconnection). Knowing the direction of the spacecraft trajectory and the sense of the dispersion reveals the general location of the reconnection site.

The second type of dispersion observed in the cusp are ion energy-pitch angle dispersions [*Burch et al.*, 1982]. Ions that have a more antiplanetward pitch angle will be observed to have higher energies than ions possessing more planetward pitch angles. The ions observed in the cusp with more antiplanetward pitch angles have already mirrored at low altitudes and therefore traveled a larger field-aligned distance from the reconnection site, compared to ions with a planetward pitch angles which have not yet mirrored. In order for this to occur, the ions with an antiplanetward pitch angle must have a higher energy so that their parallel velocity is larger, allowing them to be observed simultaneously.

The final common cusp signature is that of diamagnetic depressions in the observed magnetic field. Analysis of the diamagnetic depressions and the physics of these depressions are the focus of a future paper and are not discussed further here; however, we do use the depressions to aid detection of the cusp in this paper.

The Earth's cusp has been observed to move equatorward during times when the IMF of the solar wind turns to a southward direction [e.g., *Burch*, 1973]. This is due to an increase in reconnection rate when the shear between the IMF and geomagnetic field lines increases, so the geomagnetic field is eroded at the dayside and the open-closed field line boundary subsequently moves equatorward. The cusp is observed to move azimuthally depending on the IMF conditions [e.g., *Burch et al.*, 1985; *Candidi et al.*, 1989]. With a large B_y component in the IMF, the newly opened field lines will have a dawnward and duskward flow for the northern and southern hemispheres respectively when $B_y > 0$. The opposite is true for an IMF $B_y < 0$. The corresponding ionospheric flows also behave in a similar fashion. This is due to the convection and magnetic tension force acting in an azimuthal direction after reconnection instead of a completely poleward direction when the IMF is completely antiparallel to the dayside magnetospheric field interior to the magnetopause.

Pitout et al. [2006, 2009] undertook very large statistical investigations involving terrestrial cusp observations made by the Cluster mission. They found that the location of the cusp depends on the dynamic pressure of the solar wind as well as its IMF B_y component (as discussed previously). A seasonal effect was seen where the cusp is wider when the cusp "faces" the solar wind more directly. The northern and southern hemisphere cusp observations are centered on 12:00 local time (LT) with a range of 10:00–14:00 LT and between 75 and 80° invariant latitude. The northern cusp is more commonly located in the morning sector for negative B_y and in the afternoon for positive B_y, with an opposite trend observed in the south.

Table 1. Locations and Times of Observations for All the Cusps Presented in This Paper As Well As *Jasinski et al.* [2014] and *Arridge et al.* [2016]

Cusp Date	Time (UT)	Distance (R_S)	Latitude (deg)	Local Time
16JAN07	09:56 – 18:04	12.6	−54.5 – −43.4	10:10 – 11:39
1FEB07	15:40 – 26:46	15.6 – 16.0	−56.0 – −46.8	09:39 – 11:14
8MAR07	08:03 – 10:50	13.8 – 14.2	−43 – −40.8	11:22 – 11:42
25MAY08	01:33 – 07:47	11.6 – 9.3	56.4 – 64.4	13:16 – 14:26
24SEP08	06:15 – 07:12	10.6 – 10.3	60.6 – 62.2	12:32 – 12:41
23NOV08	06:16 – 06:47	12.2 – 12.2	62.0 – 62.7	12:53 – 12:57
3AUG08	14:47 – 22:59	11.1 – 8.2	58.7 – 72.7	12:32 – 14:55
21JAN09	11:00 – 19:00	16.5 – 15.5	42.3 – 50.4	11:37 – 12:06
14JUN13	19:40 – 22:10	14.3 – 14.6	39.8 – 37.5	10:51 – 11:02
24JUL13	00:00 – 05:30	15.4 – 15.3	51.37 – 55.03	10:28 – 11:20
17AUG13	14:00 – 16:05	18.5 – 18.4	38.0 – 33.0	10:13 – 10:22

The first confirmation of a cusp observation at Saturn occurred in the northern hemisphere [*Jasinski et al.*, 2014]. The authors reported multiple ion energy-latitude dispersions with a "stepped" structure, which have been shown to be due to "bursts" or "pulses" of reconnection occurring at the magnetopause [e.g., *Lockwood and Smith*, 1994; *Lockwood et al.*, 2001]. Analysis of the energy-pitch angle dispersions showed that the reconnection site at the Saturnian magnetopause was changing location during the observations. Two cusp observations in the southern hemisphere were reported by *Arridge et al.* [2016]. The authors also found that the southern cusp oscillates with the oscillation of the auroral oval at a period of ∼10.7 h [*Nichols et al.*, 2008]. This causes the cusp to be observed twice within ∼10 h, with the magnetosphere and field-aligned currents observed in between. On the same day as one of the cusp events presented by *Arridge et al.* [2016], further evidence for reconnection was reported with the observation of a flux transfer event [*Jasinski et al.*, 2016] in an open field line region in between the magnetosphere and magnetosheath.

Here we present other cusp observations during the Cassini spacecraft era. We present analysis and comparison of a further eight cusp traversals on 8 March 2007 (from now on referred to as "8MAR07"), 25 May 2008 ("25MAY08"), 3 August 2008 ("3AUG08"), 24 September 2008 ("24SEP08"), 23 November 2008 ("23NOV08"), 14 June 2013 ("14JUN13"), 24 July 2013 ("24JUL13"), and 17 August 2013 ("17AUG13"). With the exception of 8MAR07, all the observations were in the northern hemisphere. We will also comment and compare to observations from 21 January 2009 ("21JAN09") [*Jasinski et al.*, 2014] and the 16 January and 1 February 2007 ("16JAN07" and "1FEB07," respectively) [*Arridge et al.*, 2016].

The instrumentation used for this analysis will be described first, followed by the trajectory of the spacecraft. This is followed by an overview and description of all the cusp observations and analysis of the reconnection location and the observed plasma composition. Next, we explore possible solar wind correlations to the observations and finally present our discussion and conclusions of the survey of observations.

2. Location of the Cusp Observations

Table 1 shows all the cusp events including the 21JAN09 event reported by *Jasinski et al.* [2014] and the 16JAN07 and 1FEB07 observations reported by *Arridge et al.* [2016]. During the years of 2007 and 2008, the Cassini spacecraft performed a series of highly inclined orbits (peak absolute latitudes of >50°) where the trajectory provided the opportunity to obtain cusp observations. In 2007 high-latitude northern observations occurred in the dusk and nighttime sectors of the magnetosphere, which were less suitable for cusp detection. However, the southern part of Cassini's trajectory was suitable for cusp crossings. In addition to the southern cusp observations presented by *Arridge et al.* [2016], the other southern cusp traversal is 8MAR07. The set of Cassini trajectories in 2008 and 2013 favored northern cusp observations.

The Cassini orbits during the times that were potentially suitable for cusp observations are shown in Figure 1 and are color coded by time period. The location of the actual cusp observations is marked by similarly color-coded symbols. The cusp encounters described previously by *Jasinski et al.* [2014] and *Arridge et al.* [2016] are also indicated. Two of the events were located so close together that they cannot be distinguished in Figure 1.
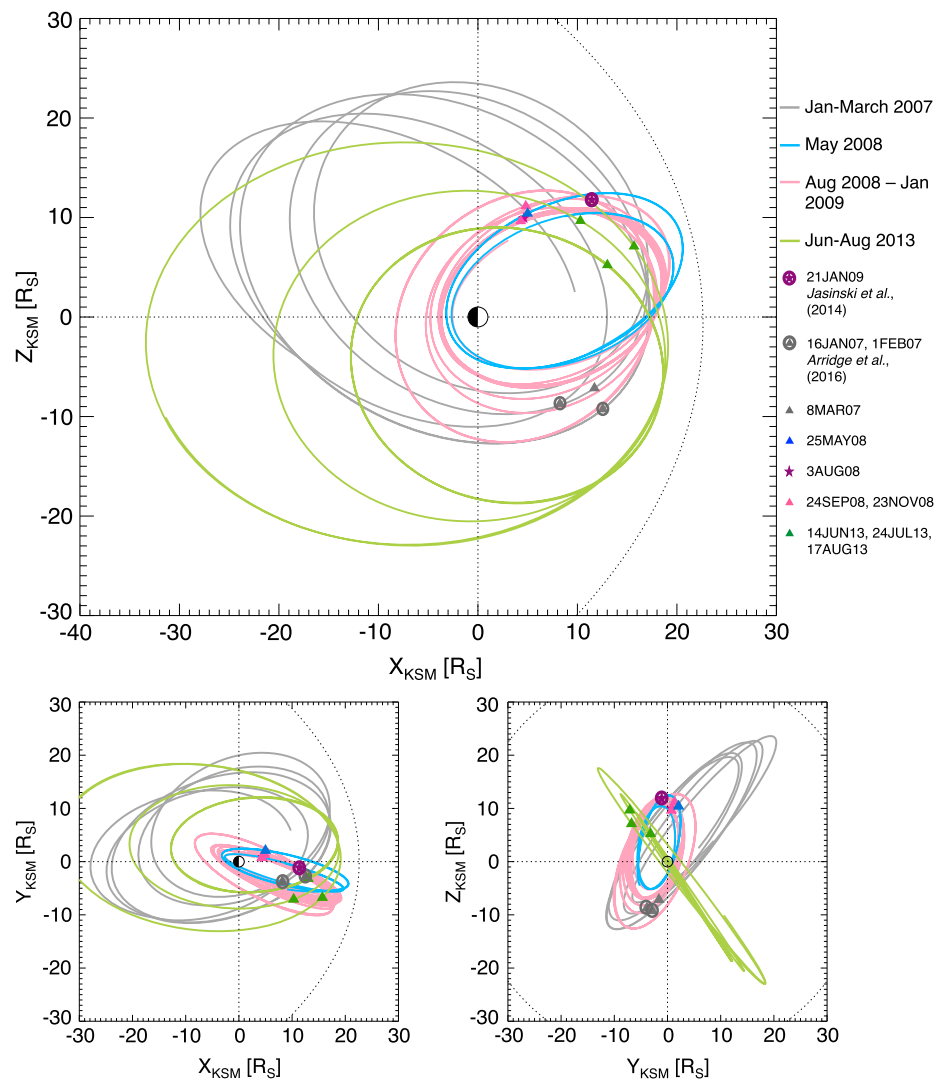
Figure 1. The trajectory of the spacecraft and locations of the cusp for the different orbits and observations. The orbit of the satellite is presented for four different time periods (shown in the legend) with the location of the cusp observation displayed as a triangle of the same color as the orbit. The 21JAN09 and 3AUG08 observations are displayed as stars to distinguish them from the 24SEP08 and 23NOV08 events, which are all located on the same set of orbits. The trajectories are presented in the Kronocentric Solar Magnetospheric (KSM) coordinate system, where X points toward the Sun, Y equals the normalized cross product of the magnetic dipole direction with X, and Z completes the right-hand set (and lies in the plane formed by X and the magnetic axis). The average magnetopause location (dotted) at $\sim$22 R_S (the lower value from the bimodal distribution found by *Achilleos et al.* [2008]) is also shown (calculated using the *Kanani et al.* [2010] model). The X-Y and Y-Z planes are shown in the bottom left and bottom right, respectively.

The trajectories were such that only one hemisphere in one quadrant (dawn-noon) was optimal to sample the cusp. In the northern hemisphere the cusp was observed at a range of altitudes and latitudes because Cassini had more trajectories that were favorable for cusp traversals. The southern hemisphere observations occurred on only one set of orbits, and therefore, all share a similar location.

3. Instrumentation

Observations from the following in situ instrumentation on board the Cassini spacecraft will be presented: low-energy electrons and ions by the electron and ion mass spectrometers (ELS and IMS, respectively) which are part of the Cassini Plasma Spectrometer (CAPS) [*Young et al.*, 2004], energetic electrons by the Low-Energy Magnetospheric Measurement System (LEMMS) which is part of the Magnetospheric Imaging Instrument (MIMI) [*Krimigis et al.*, 2004], and the magnetic field by the magnetometer (MAG) [*Dougherty et al.*, 2004].
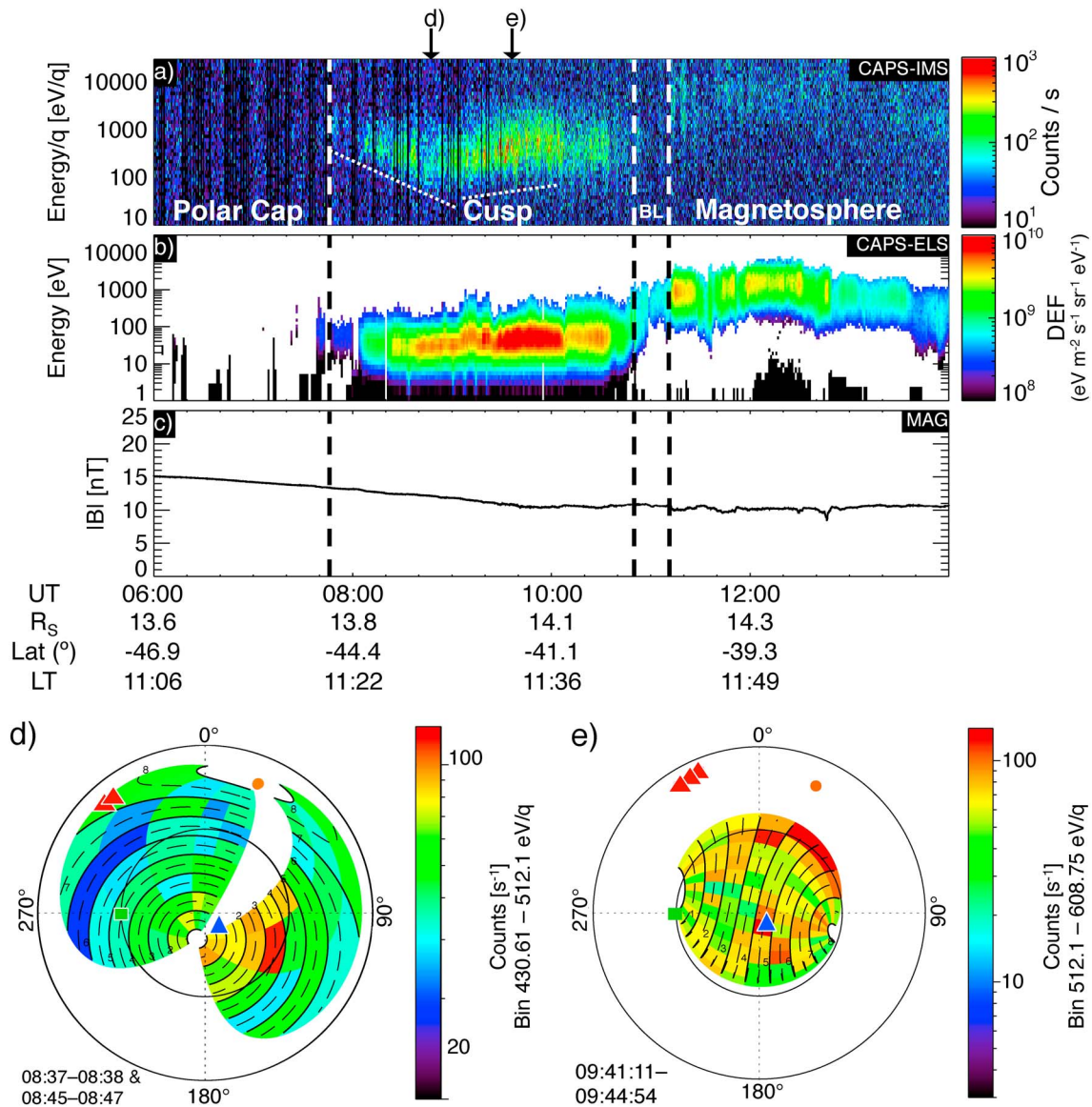
Figure 2. A high time resolution spectrogram of the ion observations from IMS displaying the two different energy-latitude dispersions (dotted and underlined in Figure 2a to guide the eye) from the (a) 8MAR07 event. (b) Omnidirectional electron differential energy flux ("DEF") from ELS. (c) Magnetic field magnitude (MAG). (d and e) The angular distributions of the ions at a point in each dispersion (the times relative to the spectrogram are shown with arrows; see text for more details). The blue and red triangles in Figures 2d and 2e represent where the ions would be observed if they were traveling in an anti-field-aligned and field-aligned directions, respectively.

ELS and IMS do not have a full 4π steradian field of view, and so the CAPS instrument is mounted on an actuating platform that moves at a maximum rate of 1°/s to increase the angular coverage and with full actuation can acquire $\sim2\pi$ sr in ~3.5 min. IMS has a time-of-flight analysis component which allows the determination of the ions mass per charge.

To describe the ion flow direction, we present the IMS data as a function of look direction about the spacecraft (example shown in Figures 2d and 2e). This is a slice of the 3-D distribution taken at a specified energy, normally corresponding to the peak count rate. The data are presented in a coordinate system centered on the spacecraft (the observer) which is facing Saturn (i.e., Saturn is at the center of the plots), with θ being a polar angle away from Saturn (0° points toward Saturn ($\boldsymbol{S}$), and 180° points directly away from Saturn). θ is represented in the plots radially away from the center, with 90° representing the inner circle and 180° representing the outer circle (and is a point in space behind the spacecraft). ϕ is an azimuthal angle measured around $\boldsymbol{S}$, where $\phi=0°$ points in the direction of $\boldsymbol{S} \times (\boldsymbol{\Omega} \times \boldsymbol{S}) = \boldsymbol{O}$, where $\boldsymbol{\Omega}$ is the spin axis of the planet. $\boldsymbol{A}$ completes the

right-handed set ($A = S \times O$). To explain this differently, if the reader can imagine that they are sitting on the spacecraft facing the planet, everything in front of them is within the inner circle (with the inner circle representing the "sides" of the observer where $\phi < 90°$ and $\phi > 270°$ is everything "above" and $90° < \phi < 270°$ is everything below the observer). Everything behind the observer is between the inner and outer circles.

The MAG data are presented in the Kronographic-Radial-Theta-Phi (KRTP) coordinate system (i.e., spherical polar coordinates). This coordinate system is spacecraft centered for the magnetic field and planet centered for the position of the spacecraft. The radial (R) vector is directed in the planet-spacecraft direction, the azimuthal vector (ϕ) is positive in the direction of Saturn's rotation, and θ completes the right-hand set ($\theta = R \times \phi$) and is in the colatitudinal direction, positive southward. In comparison to the ion flow coordinate system mentioned above, $R = -S$, $\phi = A$, and $\theta = -O$.

Also presented are solar wind properties extrapolated from 1 AU to 9 AU by the Michigan Solar Wind Model (mSWiM) [*Zieger and Hansen*, 2008].

4. Observations

4.1. Evidence for Lobe and Dayside Magnetopause Reconnection—8MAR07

The 8MAR07 event, shown in Figure 2, is very similar to the observations of the southern cusp (16JAN07 and 1FEB07) that were presented by *Arridge et al.* [2016]. Before entering the cusp, CAPS does not observe plasma above the noise level, and this region is interpreted to be magnetically connected to the planet's polar cap [*Jasinski et al.*, 2014; *Arridge et al.*, 2016].

Once in the cusp, there are two energy-latitude dispersions, underlined in Figure 2a. The first is a reverse-sense dispersion. For the first dispersion, the ions are observed to be arriving from a higher latitude and from the sunward direction (Figure 2d). A higher flux of ions are observed near the anti-field-aligned direction (blue triangle) as well as from a direction "below" the spacecraft where one would expect lobe reconnection to be occurring (the labels "d" and "e" show the time the corresponding angular distribution plots in Figures 2d and 2e correspond to in the spectrogram in Figure 2a). The second dispersion is a normal-sense dispersion, with a higher flux of ions arriving from an equatorward and a sunward direction, consistent with dayside subsolar reconnection. Therefore, the ion flow direction supports the interpretation of the location of the reconnection site from the dispersion orientation, and not an oscillation of the cusp as observed by *Arridge et al.* [2016]. Of course, without multiple spacecraft, it is not possible to determine whether reconnection in these two locations was occurring at the same time or not. The dotted lines in Figure 2a are drawn to help understand the orientations of the two dispersions which start at ~08:00 UT and end at ~10:20 UT, before a change in the plasma temperature.

The two dispersions are also accompanied by a slight energization of electrons between the two populations. Upon exiting the cusp, Cassini observed a narrow boundary layer (labeled "BL") of plasma with decreasing density and an increasing energy, before entering the magnetosphere. In all of the southern cusp events (including those presented by *Arridge et al.* [2016]), there was a boundary layer observed before crossing into the magnetosphere from the cusp. This was observed as a gradual increase (or decrease if entering the cusp from the magnetosphere) of the electron energy observed by ELS and an increase in flux of energetic electrons in LEMMS. This is interpreted to be a high-latitude extension of the low-latitude boundary layer [*Arridge et al.*, 2016].

4.2. Cusp Observation Signatures Due to "Bursty" Dayside Reconnection—3AUG08

The data obtained from the 3AUG08 cusp crossing are presented in Figure 3. Unlike the southern observations, the spacecraft was traveling planetward and poleward. There are two data gaps (in all the presented instruments) occurring at 12:10–12:50 and 16:22–18:03 UT. At the beginning of the 3AUG08 event, energetic electrons in CAPS-ELS (Figure 3a) and MIMI-LEMMS (Figure 3c) are present until 14:45 UT. The energy distribution of these electrons is similar to those observed in the magnetosphere during the 21JAN09 event, and so the plasma is interpreted to be on closed magnetospheric field lines [*Jasinski et al.*, 2014; *Arridge et al.*, 2016]. Before entering the cusp (at 14:47), the spacecraft passes through a region where the energy of the electrons is gradually decreasing and the flux of the ions increases.

From 14:47 to 23:30 UT, Cassini traversed the cusp. IMS observed a high flux of ions (Figure 3b), which had multiple energy-latitude dispersions. The data from the MIMI-LEMMS instrument (Figure 3c) show high fluxes of energetic electrons up until the cusp crossing, with a significant decrease in the first ion dispersion
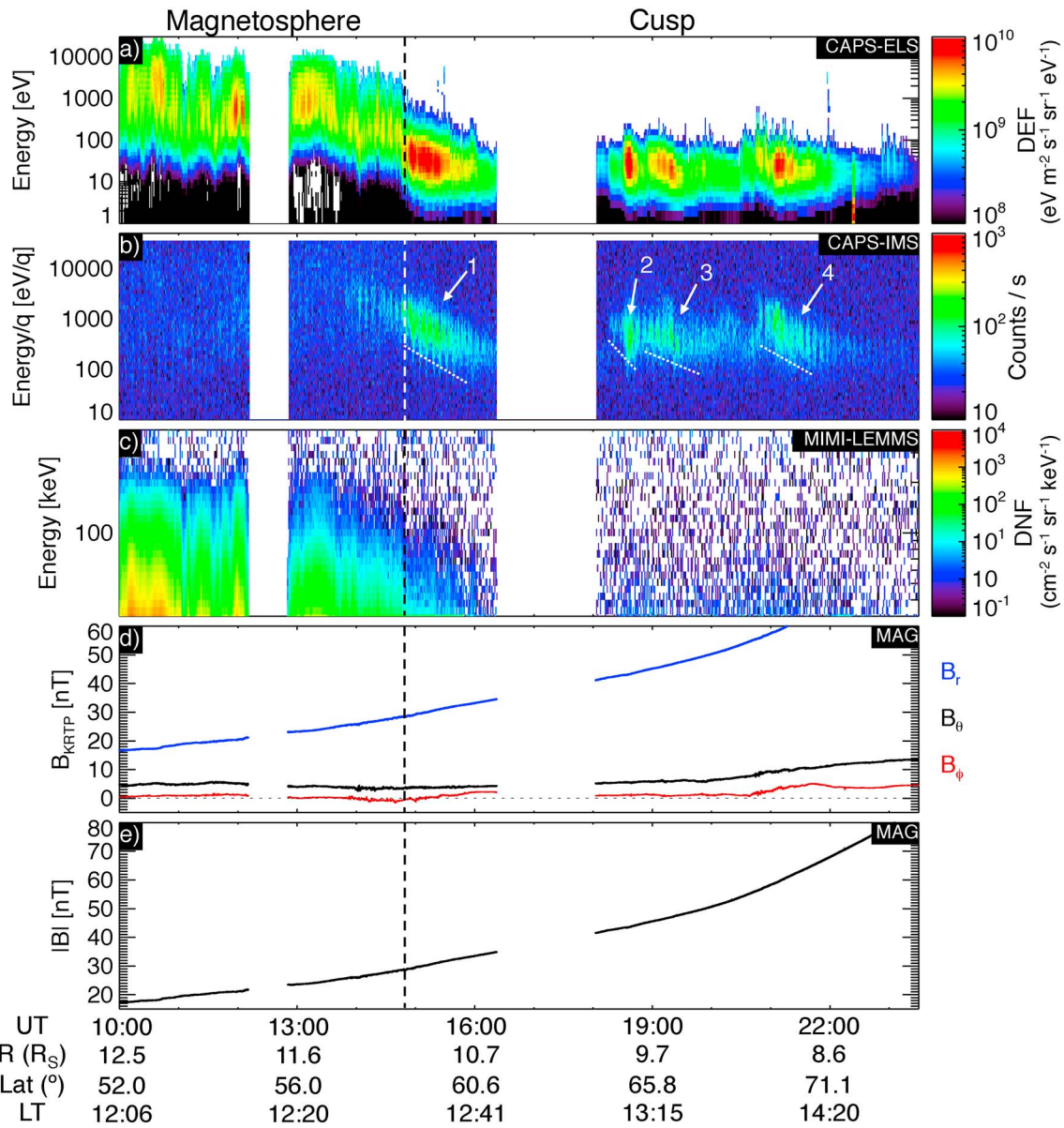
Figure 3. Observations of 3AUG08, with the cusp observed at 14:45–23:45 UT. (a) Electrons from CAPS-ELS, (b) ions (all anodes summed) from CAPS-IMS, (c) high-energy electrons from MIMI-LEMMS (the high fluxes in up to the ∼25 keV energy level are due to light contamination of the instrument), (d) the three components of the magnetic field in KRTP coordinates from MAG, and (e) the magnitude of the magnetic field also observed by MAG.

observed, followed by background levels of counts in the rest of the cusp interval. A boundary layer is observed briefly for an hour before Cassini entered cusp, where low fluxes of ions are observed as well as a slight decrease in electron energy. This is similar to the boundary layer reported by *Arridge et al.* [2016], in their observations where a field-aligned current is observed in a rotation in the B_ϕ component of the magnetic field and (here at ∼14:00 UT). The start of the cusp is marked by the clear magnetosheath-like electron low-energy fluxes at the vertical dashed line.

There are four dispersions present in the data; the first is clearly observed at 14:47–16:22 UT. The second and third dispersions are very close together, are difficult to separate, and are tentatively identified as two separate dispersions. However, the large increase in flux at ∼18:35 UT is designated to be the center of the second dispersion at 18:15–18:50, with the third dispersion occurring at 18:50–20:40. The argument that these are two separate dispersions is supported by the flux measured by ELS as well as in the IMS measurements. The electron flux, as well as the energy, increases at the start of the third dispersion in comparison to the end of

the second dispersion. At the same time there is also a step-up in the energy of ions. Both of these observations suggest that these are two separate dispersions. If this was one dispersion, the electron flux would steadily decrease (similarly to the first dispersion) and the ions would also not increase in energy. Instead, there is a clear passing of the spacecraft through two separate flux tubes filled with cusp plasma, with two different reconnection histories. All the dispersions are in the same sense, implying that the reconnection was taking place equatorward of the cusp and is also occurring in a bursty or pulsed manner [*Lockwood et al.*, 2001; *Jasinski et al.*, 2014] due to the stepped nature of the ion dispersions.

The magnetic field (Figures 3d and 3e) is almost entirely in the radial direction and is increasing significantly due to the planetward trajectory of the spacecraft. No diamagnetic depressions are seen during the cusp interval. There is a rotation in the B_ϕ component at ∼15:00 UT coincident with the start of the cusp observations. This could be due to the crossing of the open-closed field line boundary marked by a field-aligned current (FAC) [*Bunce et al.*, 2008].

4.3. Isolated Cusp — 25MAY08

Presented in Figure 4 is an observation of a cusp not directly adjacent to the magnetosphere but isolated from it by a brief traversal of the polar cap. This event (25MAY08) was observed in the northern hemisphere (Cassini traveling poleward and planetward). The 25MAY08 event starts with the spacecraft (unlike in the previous cusps) in the polar cap, with no plasma observed within the detectability threshold of the instrumentation. The 8MAR07 event also starts in the polar cap; however, what is different here is that this is a poleward pass, and the spacecraft entered the polar cap at ∼23:30 UT the previous day without seeing the cusp or a boundary layer there. The spacecraft exits the polar cap, passes through a brief boundary layer, characterized by hot and very tenuous plasma, and then proceeds through to cross the cusp.

In Figure 4, the spacecraft is already in the polar cap at 00:00 UT where electron flux was at the background level of the instrumentation. A very tenuous electron population is seen from ∼00:20 to 01:30 UT, with energies slightly higher than those in the cusp, representing a boundary layer before entering the cusp. At 01:30 until 02:30 UT the spacecraft observes dense, cold electrons in the cusp and very high fluxes of ions with the typical energy-latitude dispersion.

For the first half an hour after exiting the cusp, the spacecraft observes very low fluxes above the background, and then for the following half hour, a higher-energy population of electrons is observed in ELS and LEMMS (the high fluxes below ∼25 keV just after 05:00 and 08:30 UT are light contamination in the LEMMS instrument). Upon reentering the cusp at 03:30 UT, the higher-energy electrons continue to be observed for almost an hour in the cusp. There are a few bursts of increased flux in the plasma, the largest being associated with a small magnetic depression at ∼04:10 UT. There is a clear energy-latitude dispersion, with a gradual decrease in flux. At 06:40 UT, there is another dispersion with an increase in ion energy observed, before the cusp is exited at ∼09:00 UT and the spacecraft reenters the polar cap.

Prior to 04:00 UT, the actuator was actuating only very slowly or not at all, so ion angular distributions are not available for the first dispersion event. At 04:00 UT full actuation resumed. Panel (ii) presents the angular distributions of the ions during the second cusp dispersion, showing that the maximum ion flux was coming from the direction "below and behind" the spacecraft, consistent with travel inward along a reconnected field line as it is pulled northward through the cusp. The isolated nature of the cusp could hence be explained by an onset of reconnection after the spacecraft crossed the open-closed field line boundary.

4.4. Tenous Cusp Observations — 24SEP08 and 23NOV08

These two observations have been grouped together due to the similarity in the ELS and IMS data and the relevant observations having short timescales. The data for the 23NOV08 observations are presented in Figure 5, and those for the similar event 24SEP08 are shown in the supporting information. Before the cusp observation in Figure 5, the spacecraft (similar to previous cusp intervals) crossed a boundary layer, where the energy of the electrons gradually decreased (observed by ELS and LEMMS, Figures 5a and 5c). The determination of the composition of the ions is difficult due to the low count rate and small number of time of flight accumulations available. However, in the magnetosphere (03:54–05:36 UT) the water group percentage (of H^+) was $5.3 \pm 0.4\%$, which decreased to $1.3 \pm 0.2\%$ in the overlapping bin (05:36–06:27 UT). There were no W^+ counts above the background level in the cusp.

The start of the cusp observations was at 06:15 UT (for both events). High-energy electrons are not observed in MIMI-LEMMS (Figure 5c) during the 23NOV08 cusp crossing, but during the 24SEP08 observation they are.
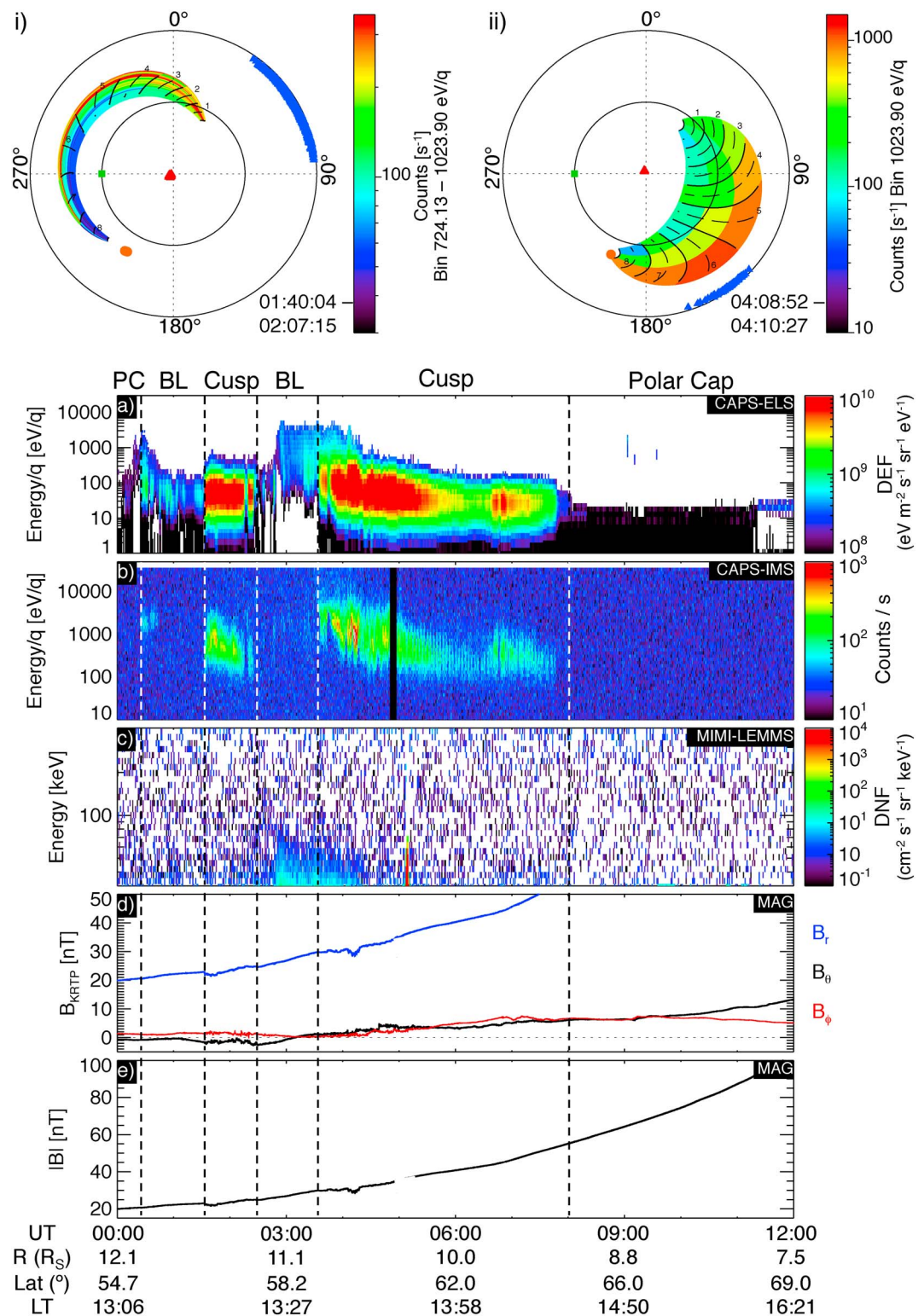
Figure 4. Observations from 25 May 2008, with the cusp observed at 01:30–02:30 and 03:30–07:45 UT. (i and ii) The ion angular distributions during the first two ion dispersions. (a) Electrons from CAPS-ELS, (b) ions from CAPS-IMS, (c) high-energy electrons from MIMI-LEMMS, (d) the three components of the magnetic field in KRTP coordinates from MAG, and (e) the magnitude of the magnetic field also observed by MAG.
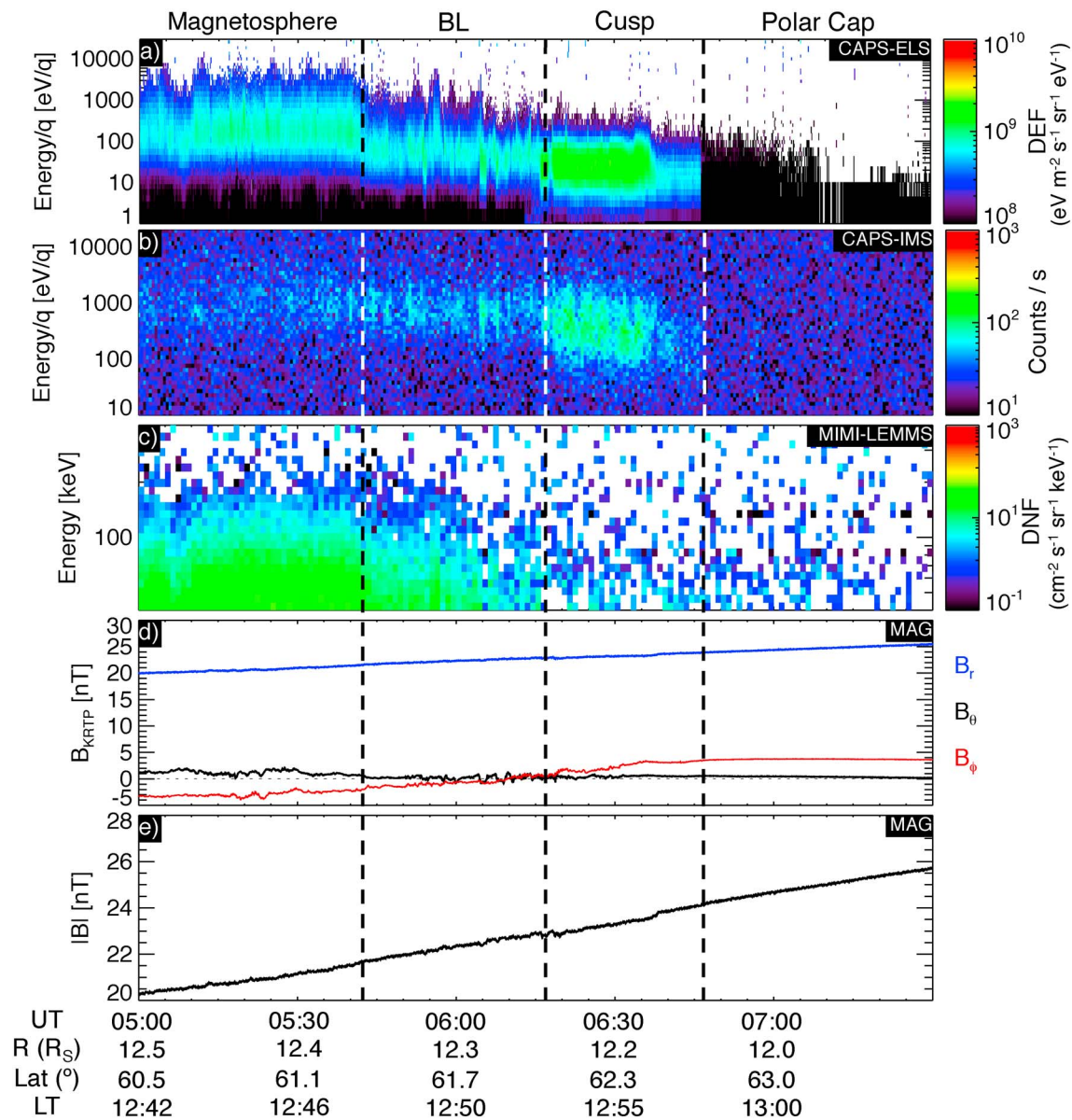
Figure 5. Observations of the 23NOV08 event, with the cusp observed at 06:15–06:45 UT. This figure is in the same format as Figure 3.

Two pulses of increased electron flux are observed bounding the cusp observations. This is the same as previous energetic electron observations on open field lines [*Roussos et al.*, 2015; *Mitchell et al.*, 2016; *Palmaerts et al.*, 2016], the reason for which previous reports have been unable to explain, but have shown that they are most likely triggered by reconnection.

In both days, the cusp observations do not last longer than approximately 30 min. The September observation has a data gap, and the actual data are collected for no more than 10 min. However, the electrons are already lower in energy before the data gap occurs, implying that Cassini may already be in the cusp during the time of the data gap. Assuming that the spacecraft is in the cusp during the data gap, the cusp interval would be approximately 20 min in duration.

The 23NOV08 observations show a weak "normal-sense" ion dispersion, with high energies observed at lower latitudes, indicating reconnection occurring at the dayside subsolar magnetopause (Figure 5). The 24SEP08 observation does not show any significant dispersion. The magnetic field orientation for both observations is the same, very strongly in the radial direction.

4.5. Northern 2013 "Summer" Cusp

The CAPS instrument was switched off permanently in 2012, due to a short circuit. Therefore, there are no low-energy particle observations for the high-latitude orbits in 2013, and so another source of data must be a base for the search for the cusp during this period. MAG is used to locate magnetic field depressions which have been observed frequently at the terrestrial cusp as well as in some previous Saturn cusp examples including those presented by *Jasinski et al.* [2014] and more noticeably *Arridge et al.* [2016]. Depressions are not observed in the 3AUG08, 24SEP08, and 23NOV08 observations. This is due to their low radial distances ($\sim$8–12 R_S) from the planet, making the field more difficult to depress, as well as very low density plasma present in the 24SEP08 and 23NOV08 cusps. However, the orbits during 2013 had large radial distances ($>$14 R_S) where the cusp would most likely be observed, making it more likely that a detectable field depression would occur, if the cusp is traversed.

A study of the MAG data reveals three events with magnetic depressions in the cusp which will be described in this section (14JUN13, 24JUL13, and 17AUG13). All three northern observations occur with the spacecraft traveling equatorward in the prenoon region and are in the middle- to high-altitude range (14–18 R_S). An overview of the 14JUN13 cusp will be presented, followed by a description of the other events. The observations of the 24JUL13 and 17AUG13 events can be found in the OSM.

The cusp was identified using a combination of the MAG and LEMMS instruments. First of all, a decrease in magnetic field strength greater than any gradual change of the magnetic field strength (due to the spacecraft trajectory) identified the diamagnetic depression. Once a depression was located, the energetic electron observations from LEMMS were used to determine whether there was a decrease in (or a complete lack of) flux, similar to previous cusp examples. A magnetic depression with no energetic particles would provide evidence that there is a plausible plasma population below the LEMMS detectability threshold present (that would have been observed by CAPS had it still been activated) that is depressing the magnetic field.

The data from the 14JUN13 observation are presented in Figure 6, where the high-energy electron (Figure 6a) and magnetic field (Figures 6b and 6c) data are shown. Before entering the cusp (identified for this example as the region of significant field depression), the spacecraft largely observes counts at the noise level for the energetic electron measurements, with a burst of electrons occurring just before the cusp at 18:50 UT, which coincides with a small rotation in the B_ϕ component of the magnetic field. The magnetic field depression starts at 19:40 UT (with a field strength of $\sim$11.5 nT). At 21:00 UT, the depression reaches a minimum field strength of $\sim$8.5 nT. At 21:40, there is local drop in the magnetic field ($\sim$1 nT), and a burst of high-energy electrons, which is interpreted as a brief entry into the boundary layer between the cusp and the magnetosphere (similarly observed in the 25MAY08 encounter), before reentering the cusp.

The cusp is exited at 22:10 UT, where the spacecraft enters a boundary layer of increased flux of energetic electrons. At 22:35 UT there is a clear crossing into the magnetosphere where LEMMS observes the highest fluxes of energetic electrons in this event. Passage deeper into the closed field region is also marked by a slow rotation in B_ϕ which could be the observation of a field-aligned current inward of the open-closed field line boundary. The B_ϕ rotation is also clearly seen upon entering the boundary layer at $\sim$22:05 UT.

Contrastingly, in the 24JUL13 event, it is not clear where the open-closed field line boundary is because there is no increase in flux of electrons observed in LEMMS when exiting or entering the cusp. This is similar to the 25MAY08 event, where the cusp appears to be "isolated" in the polar cap. In the 24JUL13 we identify the cusp as the interval where the magnetic field is depressed. The cusp has a strong magnetic field depression, and there are short bursts ($\sim$30 min) of increased flux an hour and 2 h before the start of the cusp.

The 17AUG13 cusp observation is, in a manner, the opposite of the 24JUL13 observation because it is bounded on both sides to the magnetosphere. There is a boundary layer observed for $\sim$4 h before and $\sim$2.5 h after the cusp interval, with slightly lower fluxes of energetic electrons than the magnetosphere. Whereas the magnetic field depression in the 14JUN13 observation is gradual, the 24JUL13 and 17AUG13 observations both have large erratic changes in their depressions, which would probably be due to density changes in the low-energy plasma. During the first half of the 17AUG13 magnetic field depression, there are background levels of electrons observed in LEMMS which is similar to the 2007 cusp observations and would imply that the depression is not centered on the cusp but on the boundary layer adjacent to the cusp. We identify the cusp in this example as the region with the lowest energetic-plasma fluxes observed by MIMI-LEMMS, as well as containing part of the depression. The boundaries have a rotation in the B_ϕ component of the magnetic field, marking
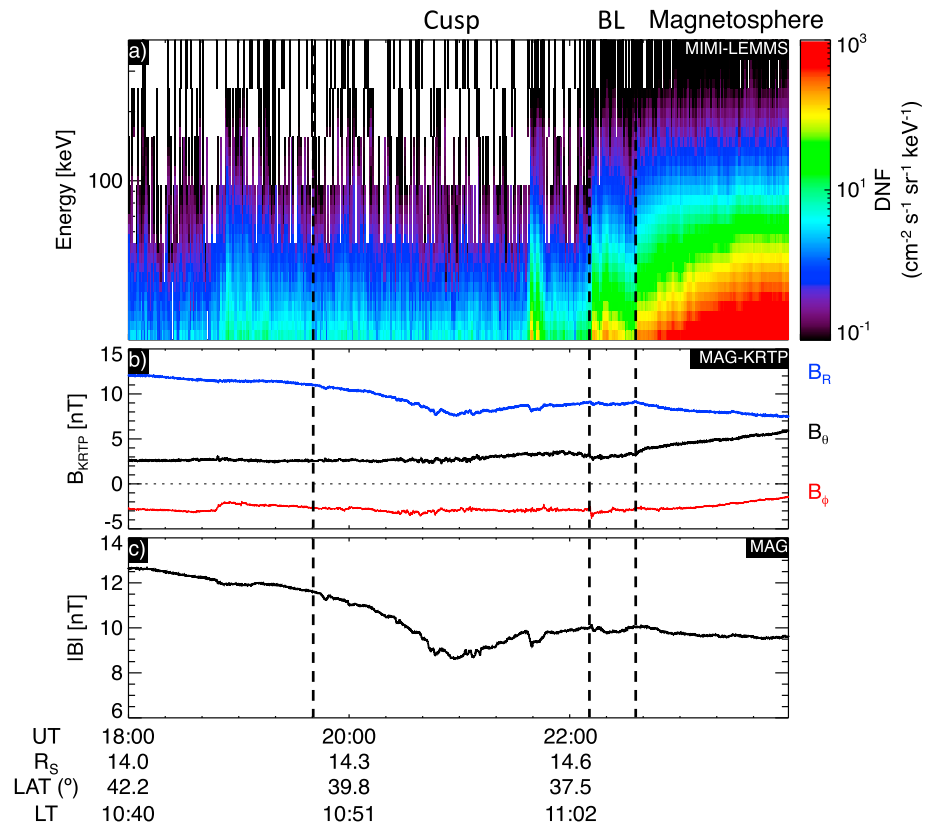
Figure 6. Observations from 14 June 2013, with the cusp observed at 19:40–22:35 UT. (a) High-energy electrons from MIMI-LEMMS, (b) the three components of the magnetic field in KRTP coordinates from MAG, and (c) the magnitude of the magnetic field also observed by MAG.

what we interpret to be the open-closed boundary with the magnetic signature of a FAC [e.g., *Bunce et al.*, 2008; *Jasinski et al.*, 2014; *Jinks et al.*, 2014]. The depressions observed by Cassini are not always centered on the cusp; this is discussed in detail in a future paper led by J. M. Jasinski.

5. Energy-Pitch Angle Dispersions and Calculating the Distance to the Reconnection Site

For observations when CAPS was functioning, ion energy-pitch angle dispersions were observed in the IMS data while in the cusp. From these energy-pitch angle dispersions the distance to the reconnection site is determined for the cusp observations, by fitting the *Burch et al.* [1982] model to the IMS energy-pitch angle data using the following equation:

$$E\left(\alpha_o, t\right) = \frac{m}{2t^2}\left[\int_{s_i}^{s_o} ds/\sqrt{1 - sin^2\alpha_o\left(B(s)/B_o\right)}\right]^2 \tag{1}$$

where E is the energy of the ion, ds is the arc length along a model field line, s_o and s_i are the observation and injection points, respectively, m is the particle's mass, $B(s)$ is the magnetic field strength along the field line, B_o is the magnetic field strength at the observation point, α_o is the observed pitch angle, and t is the transit time of the particle from the injection site (via the mirror point for ions that have mirrored) to the observation point. Both $B(s)$ and B_o are obtained from the *Khurana et al.* [2006] magnetospheric field line model. The solar wind dynamic pressure obtained from mSWiM for each event is used as an input for generating the *Khurana et al.* [2006] model, as well as the location of Cassini to extract B. mSWiM cannot propagate the IMF orientation of the upstream solar wind, so the IMF input for the Khurana model is not changed between events and is set to be in the northward direction.
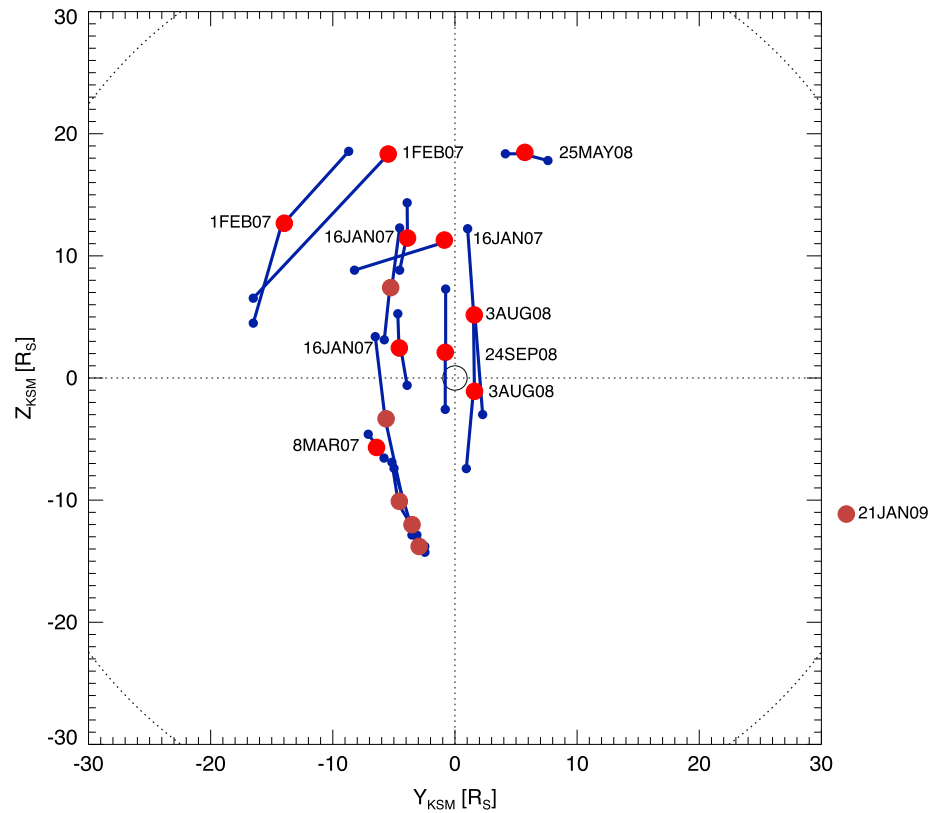
Figure 7. A projection of the estimated locations of reconnection from the calculated field-aligned distances (using the energy-pitch angle dispersions and the *Burch et al.* [1982] model) are shown in red and associated errors in blue. The plot is in the *Y-Z* KSM plane (as viewed from the Sun) with the sunlit planet in the center and an average model magnetopause location (dotted) also shown (calculated using the *Kanani et al.* [2010] model and the compressed standoff distance value (22 R_S) from the bimodal distribution found by *Achilleos et al.* [2008]).

The model was fit to the data using the Levenberg-Marquardt nonlinear least squares algorithm [*Markwardt*, 2009]. If the dispersion was not clear, the signal-to-noise ratio was low or the model was unable to be successfully fitted, a calculation could not be made. However, for the successful fits, the results were all binned together within the same energy-latitude dispersions, with the errors propagated, to give a final value for the distance to the reconnection site and its uncertainty.

The 25MAY08 result shows a distance to the reconnection site of $16 \pm 3\ R_S$ (for the second dispersion) which is similar to that calculated for 8MAR07 of 16 ± 1 and $15.6 \pm 0.4\ R_S$. These imply a reconnection site poleward of the subsolar point. 24SEP08 produced a reconnection distance of $21 \pm 5\ R_S$, similar to the 3AUG08 results of 32 ± 7 and $26 \pm 8\ R_S$ (for the first two dispersions), which reveal sites closer to the subsolar point, and more similar to the reconnection location reported for 21JAN09 [*Jasinski et al.*, 2014]. No results could be obtained for 23NOV08. A full table of the results can be seen in the OSM.

The calculated field-aligned distances were traced along field lines using the *Khurana et al.* [2006] magnetospheric field line model, and the location of the reconnection site was estimated. The results can be seen in Figure 7, where the locations are shown as if viewed from the Sun in the *Y-Z* plane (in the KSM coordinate system). The estimated sites (for reconnection) occur over a large range of locations, including low and high latitudes. The large calculated field-aligned distances (~50 R_S) for the 16JAN07 and 1FEB07 events (as well as the latter calculations for 21JAN09) are more feasible with an expanded magnetosphere. For the 16JAN07 and 1FEB07 events, if lower projections for the solar wind dynamic pressure were to be used (than the solar wind model predicts), then these locations would move equatorward. The distribution of the reconnection locations is largely centered slightly poleward (toward the north) of the subsolar point, with only the 21JAN09 event located very far south of the subsolar point.

6. Plasma Composition in the Cusp

When analyzing the ion composition in the cusp and the adjacent magnetosphere using IMS, two ratios for comparison can be used: a mass per charge of 2 amu/q to ionized hydrogen ratio ([m/q = 2]/H^+) and ionized water group to hydrogen ion ratio (W^+/H^+). The water group ions include O^+, OH^+, H_2O^+, and H_3O^+. The water group originate principally from Saturn's icy moon Enceladus (as well as the other icy moons), and therefore, we expect higher percentages of these ions in the magnetosphere in comparison to plasma entering the cusp from a magnetosheath origin. Both He^{++} and H_2^+ have a mass per charge of 2, but we would expect the ions to be H_2^+ in the magnetosphere with approximate percentages relative to H^+ of ∼10–20% or more, peaking at a distance of Titan's orbit (20 R_S) [*Thomsen et al.*, 2010] which is predicted to be the source of these ions [e.g., *Cui et al.*, 2008]. Titan is the dominant source, but water from Enceladus, Rhea, and Saturn's rings also contributes to the H_2^+ found in the Saturnian magnetosphere [*Tseng et al.*, 2011]. Cold H_2^+ and W^+ have higher concentrations at the equator, contained there due to centrifugal forces, therefore reducing the abundances at higher latitudes [*Persoon et al.*, 2009]. However, lower abundance values for m/q = 2 ions would suggest that they are He^{++} of a solar wind origin (∼4%) [e.g., *Ogilvie et al.*, 1989]. The data reduction software written by *Reisenfeld et al.* [2008] is used to produce the ion counts from the time-of-flight composition data from IMS.

The magnetosphere adjacent to the cusp has a variety of W^+/H^+ percentages ranging from 3.5 ± 0.2% (16JAN07) to 32.6 ± 1.2% (3AUG08). These percentages are much lower in the cusp with the lowest being 0.29 ± 0.02% and the highest 1.3 ± 0.2% (25MAY08 and 23NOV08, respectively). The [m/q = 2]/H^+ in the magnetosphere adjacent to the cusp has percentages from 8.3 ± 0.27% to 28.2 ± 0.1% (8MAR07 and 3AUG08, respectively), suggesting that these ions are H_2^+. In the cusp these [m/q = 2]/H^+ values are lower, ranging between 1.5 ± 0.05 and 4.76 ± 0.03 (8MAR07 and 3AUG08, respectively), which suggest that this component of the plasma is He^{++} and of a solar wind origin. A full table of the compositional analysis can be seen in the OSM.

7. Survey of Upstream Conditions Using mSWiM

Unlike at the terrestrial magnetosphere, where there are spacecraft upstream of the magnetosphere observing the conditions in the solar wind (SW), it is a lot more difficult to correlate SW changes to processes in the magnetosphere with a single spacecraft such as Cassini. Therefore, solar wind propagation models are used as proxy upstream monitors for Saturn's magnetosphere. mSWiM is an MHD model of predicted solar wind conditions at various bodies of interest, propagated from spacecraft observations at 1 AU, from either Earth, STEREO A or STEREO B spacecraft [*Zieger and Hansen*, 2008]. The most accurately predicted solar wind property of the model is the solar wind velocity, followed by the magnitude of the IMF and density. Ideally, one would also like to use the normal component (in RTN coordinates) of the IMF (B_{Normal} is the component closest to a planetary Z axis) to test whether reconnection is controlled by the orientation of the IMF as for the Earth. However, B_{Normal} is very inaccurate having shown insignificant correlation between model and observations. The propagations are most accurate for observations where the selected spacecraft near Earth orbit (at 1 AU) and Saturn were aligned within 75 days of apparent opposition. It has been shown that the uncertainty in predicted arrival time near apparent opposition is ±15 h. Propagations outside these alignments (75 days) are not as accurate but are, however, still statistically significant [*Zieger and Hansen*, 2008].

The following events occur within 75 days of apparent opposition: 16JAN07 (54 days from apparent opposition), 1FEB07 (38 days), 8MAR07 (3 days), 25MAY08 (38 days), 21JAN09 (31 days), 14JUN13 (17 days), 24JUL13 (53 days), and 17AUG13 (69 days). The following events occurred outside 75 days of apparent opposition: 3AUG08 (108 days), 24SEP08 (150 days), and 23NOV08 (90 days).

The solar wind dynamic pressure (P_{RAM}) indicates whether the magnetosphere is being compressed, while a high Alfvénic Mach number, M_A (dependent on low magnetic field strengths, high densities, and high velocities), in the solar wind would produce a high-β magnetosheath, making it more likely for reconnection to be suppressed and to only occur when the magnetic field lines are near completely antiparallel [*Slavin et al.*, 1984; *Masters et al.*, 2012]. The results are presented in Figure 8, with P_{RAM} and M_A presented in black and red, respectively, for 10 days on either side of each event (except for 16JAN07 and 1FEB07 which are presented together in Figure 8a). The number of days from apparent opposition can be found in brackets for each observation.

For almost half of the cusp observations (16JAN07 and 1FEB07 (Figure 8a), 24SEP08 (Figure 8e), 23NOV08 (Figure 8f), and 24JUL13 (Figure 8i)) there is a significant increase in the ram pressure, especially for 24SEP08
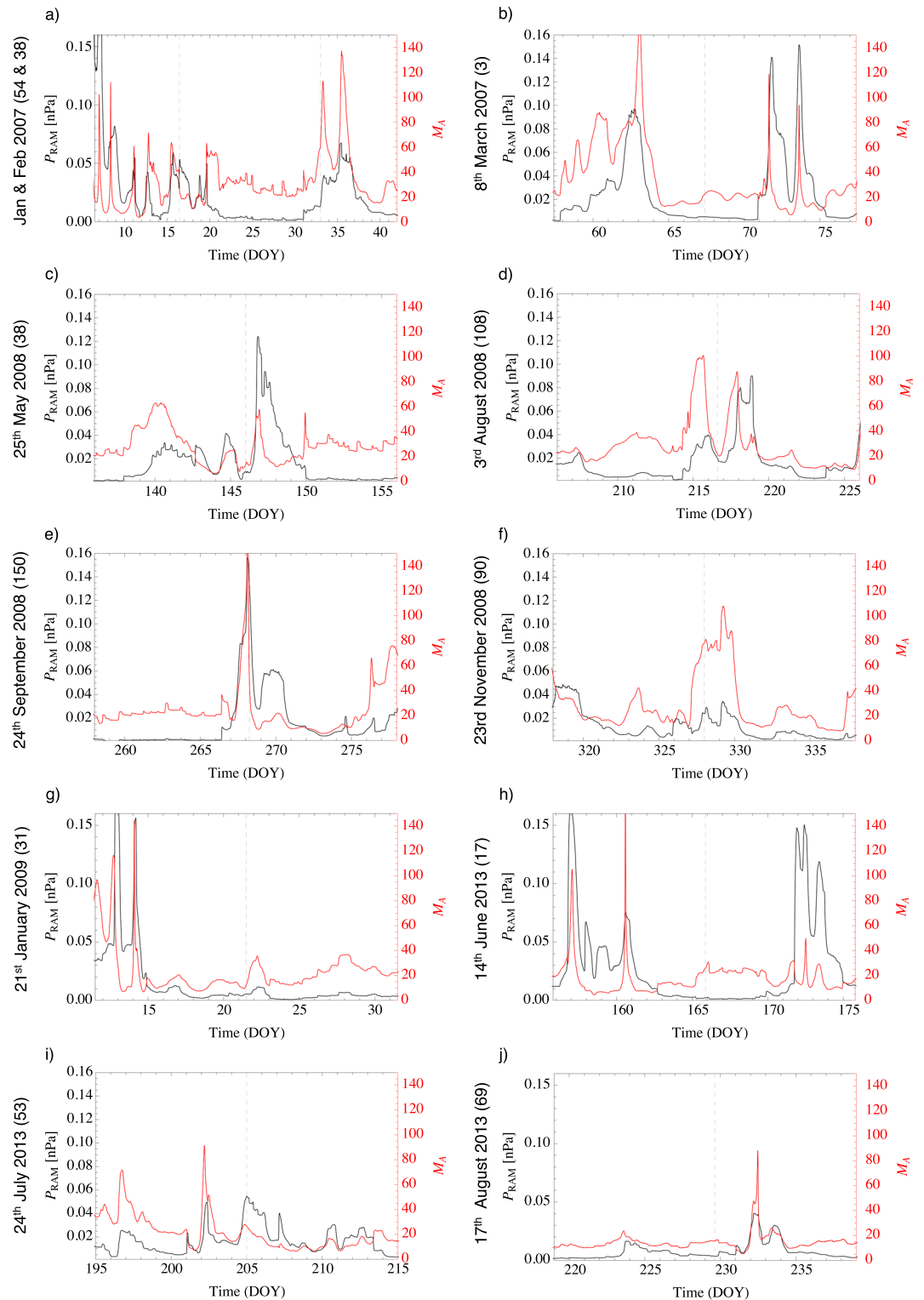
Figure 8. mSWiM propagations of the upstream solar wind conditions at Saturn for 10 days before and after the cusp observations (with an uncertainty of 15 h). The ram pressure (P_{RAM}) and the Alfvénic Mach number (M_A) are presented in black and red, respectively. The number of days since apparent conjunction is shown in brackets next to each observation. The dashed line represents the start of the cusp observation. The day of year is labeled as "DOY."

which has the largest peak of ~0.15 nPa. These would correspond to large compressions of the magnetosphere, which have been shown to provide more favorable conditions for dayside reconnection [e.g., *Jackman et al.*, 2004]. However, it is also important to note that two of these days also have the longest separation from apparent opposition (all >75 days).

Three of the other six days (8MAR07, 25MAY08, and 21JAN09) do not occur during peaks, but they do occur during modest increases in ram pressure. 25MAY08 is at the start of a large pressure increase, with a modest increase having already occurred. However, the increases for 8MAR07 and 21JAN09 are extremely modest and less significant. The other three days occur during periods of very low predicted ram pressures.

It is interesting to see that for 16JAN07, 1FEB07, 24SEP08, and 23NOV08, M_A is at a peak or very large (>40), meaning that the reconnection that occurred to produce the entry of solar wind plasma through the cusp must have occurred at a location on the magnetopause where the magnetic shear was very large. The lowest M_A of ~10 was observed for 21JAN09. For the other five observations M_A was modest, averaging ~20 and did not occur during significant peaks or troughs. This supports the conclusion that cusp detections can be found during both compressed and more expanded conditions as reported by *Arridge et al.* [2016].

8. Discussion and Conclusions

Complementing the three cusp observations (16JAN07, 1FEB07, and 21JAN09) previously reported [*Jasinski et al.*, 2014; *Arridge et al.*, 2016], a further eight more cusp observations in the in situ data have been presented. The 16JAN07 and 1FEB07 events both observed the cusp twice, which brings the total of cusp crossings to 13. The observations display considerable variability, with different types of energy dispersions and plasma conditions observed, various upstream solar wind conditions, and a disparity in the strength of diamagnetic depressions.

Eleven of these crossings are adjacent to a boundary layer of mixed plasma before entering the magnetosphere and are similar to terrestrial observations [e.g., *Dunlop et al.*, 2005]. The outbound crossings of the second cusps in 16JAN07 and 1FEB07 (which have the magnetosphere on both sides of the observation), however, do not have a boundary layer and instead pass directly into the magnetosphere. In contrast, the 17AUG13 observation does have a boundary layer present on either side of the event.

The ion compositions in the cusp and the adjacent magnetosphere show that the [m/q = 2]/H$^+$ ratio is much higher in the magnetosphere ($8.3 \pm 0.27 - 28.2 \pm 0.1$) which is in agreement with other studies that suggest that this region contains H_2^+ [*Thomsen et al.*, 2010]. In the cusp this ratio is much lower (average of 2.8 ± 0.2) which is similar to solar wind observations and therefore the m/q = 2 ion is more likely to be He^{++}. The average He^{++} to H$^+$ abundance ratio in the solar wind is ~3% and ~5% at solar minimum and maximum, respectively [*Ogilvie et al.*, 1989], which is similar as the values found in the cusp. These authors reported very occasional abundance ratios of He^{++}/H$^+$ of ~10%; however, these occurrences are very rare. The water group to proton (W$^+$/H$^+$) ratio is also much higher in the magnetosphere in comparison to the cusp, as expected (the moon Enceladus is the main source of water group ions). Some nonzero values of W$^+$ are found in the cusp, which is interpreted to be plasma that has not drained out of the newly opened flux tubes.

8.1. Ion Energy-Latitude Dispersions
The variety of the characteristics of the plasma observations suggest different processes ongoing during the different cusp observations. The most striking is the first observation of lobe reconnection occurring during 8MAR07 (Figure 2). A reverse-sense ion energy-latitude dispersion is observed. This is then followed by a normal-sense dispersion. This is the only example we present which has reconnection occurring at two different locations during the same cusp interval.

Multiple ion energy-latitude dispersions are observed during the 25MAY08 event. The presence of magnetospheric plasma (high-energy electrons in Figures 4a and 4c) between the first and second dispersions shows that this may be a temporal observation of the cusp motion over the spacecraft, and not two separate cusps. A similar observation was found at Earth [e.g., *Zong et al.*, 2008; *Escoubet et al.*, 2013], where a double cusp was observed, and was shown to be the motion of the cusp due to a change in the IMF orientation. *Wing et al.* [2001], however, have shown that two cusp regions can be present simultaneously at Earth. Without multiple spacecraft to test whether the cusp has moved, this hypothesis cannot be verified.

However, the continuous observation of the cusp during the second and third consecutive dispersions is different to that reported above (at Earth). The multiple dispersions here are not due to a motion of the cusp because there is no change in the ion dispersion direction. If the cusp had moved, the ion energy would be gradually dispersed in the opposite sense on neighboring intervals. However, there is a "step-up" in the energy which shows that "pulsed" reconnection is also occurring on this day. The 3AUG08 event also displays multiple dispersions, similar to the 21JAN09 event [*Jasinski et al.*, 2014]. The changes in the plasma regime while in the cusp, as well as "step-like" energy-latitude dispersions in the ion observations, suggest that reconnection is pulsed at the magnetopause, and not steady [*Lockwood and Smith*, 1994]. The locations of the 25MAY08 and 3AUG08 events are very similar, and the energy-pitch angle analysis reveals a similar field-aligned distance to the reconnection site. This finding indicates the possibility that the same area of the magnetopause is being reconnected for these two events. The 25MAY08 and 24JUL13 observations differ from all the others in that the spacecraft is already on open field lines mapping to the polar cap prior to entry into the cusp. In the other cusp observations, however, there is a definite transition from magnetospheric plasma on closed field lines to the cusp plasma on open field lines. This comparison shows that the spacecraft is already traversing open field lines at the start of the observations for 25MAY08 and 24JUL13. This suggests that there is motion of the cusp and magnetospheric field lines over the spacecraft.

The cusp event most similar to 21JAN09 [*Jasinski et al.*, 2014] is the 3AUG08 observation. The trajectory for 3AUG08 explores a greater region of local time in comparison to 21JAN09, and so the observations show that the cusp is spread in local time. Therefore, the energy-time dispersions for 3AUG08 are more likely to contain an element of azimuthal dispersion as the open field line subcorotates, as well as the usual poleward dispersion associated with analogous events at Earth. The Earth's cusp can also be spread in local time when there is a strong B_y component of the IMF. However, without accurate solar wind data at Saturn, this cannot be investigated further. For the 21JAN09 event, where a subsolar reconnection site is predicted, it is much more likely that azimuthal convection at Saturn is the cause. If the IMF has a large B_y component, then reconnection will most likely be suppressed [*Masters et al.*, 2012], at the subsolar point. Reconnection will most likely occur when there are large local shear angles (so a small B_y component), decreasing the likelihood that the azimuthal motion is due to the IMF B_y. However, as the magnetosheath magnetic field is draped along the magnetopause, reconnection could occur away from the subsolar point where the IMF field has a B_y component, and therefore, azimuthal motion of the cusp could be occurring similarly to Earth observations. *Badman et al.* [2013] have previously reported reconnection occurring with the IMF having a B_y component.

The 24SEP08 and 23NOV08 events both present very tenuous plasma observations. The low ion counts make it difficult to discern an energy-latitude dispersion. There is a possible dispersion in the 23NOV08 event, but the low signal to noise makes it inconclusive. These two observations are very similar to each other but not to the other events. One of the reasons that these observations are so short in duration could be that the spacecraft traversing the cusp with a large impact parameter. The other could be that reconnection had only just occurred at the magnetopause, and so the spacecraft entered the polar cap quite soon after the start of the cusp.

8.2. Location of Magnetic Reconnection

The field-aligned distance to the reconnection site was calculated for each energy-pitch angle dispersion and has produced a varied set of results. The results had a range of values of 16 ± 1 to $51 \pm 2\,R_S$. The median value was 29.5 R_S, and the lower and upper quartile values were 18.5 and 47.5 R_S, respectively. The results show that reconnection occurred at various areas along the magnetopause, with most of the events having reconnection locations poleward of the subsolar regions. This is in agreement with *Desroche et al.* [2013] who modeled the regions more likely to be reconnected along the magnetopause (as well as independent MHD simulations of the IMF effect on Saturn's magnetosphere by *Fukazawa et al.* [2007]) and showed that such regions would be generally poleward of the subsolar point. As mentioned above, most of the calculated reconnection sites are in agreement with *Desroche et al.* [2013], but most of the 21JAN09 as well as the 8MAR07 reconnection locations lie outside the predicted areas found by *Desroche et al.* [2013] (i.e., southward of the subsolar point). However, the simulations by *Desroche et al.* [2013] are for southern summer conditions (only three of our events are during this time) as well as for local IMF orientations only near the ecliptic plane. Without knowledge of the upstream IMF, it is difficult to make any more detailed comparison between their predictions and our calculated reconnection locations for 8MAR07 and 21JAN09. Our results are similar to the model reconnection locations for a northward IMF presented by *Masters* [2015]. Our results agree with *Masters* [2015] and show that the cusp maps to reconnection sites occurring over a wide range of locations along the magnetopause.

8.3. Solar Wind Correlation

All of the cusp observations have been compared to the propagated upstream solar wind data from the propagation model, mSWiM. Eight (16JAN07, 1FEB07, 24SEP08, 23NOV08, 24JUL13, 21JAN09, and 25MAY08) out of 11 cusp events occurred during increases in the ram pressure of the solar wind to within 15 h, five of which occur during significant peaks, while the other three coincide with modest increases in ram pressure. It is worth noting that two of these events occur 75 days after apparent opposition, and so the propagated parameters are less accurate [*Zieger and Hansen*, 2008]. An increase in ram pressure produces a compression of the magnetosphere which has been shown to provide more favorable conditions for reconnection to occur [*Jackman et al.*, 2004]. Three of these eight observations also do not have high Alfvénic Mach numbers (M_A), resulting in a lower β magnetosheath. Hence, for the other observations with high M_A, the reconnection that led to the cusp events must have occurred at a location on the magnetopause where the local magnetic shear was extremely large, i.e., close to 180° [*Slavin et al.*, 1984; *Masters et al.*, 2012]. Of the other four observations that do not coincide with increases in ram pressure, only one (17AUG13) had an M_A of ≤ 20. The other three did not occur during peaks or troughs in M_A. The B_{Normal} component of the IMF is not presented as it is the least accurate of the variables produced by mSWiM, and therefore, it is not possible to correlate the orientation of the predicted IMF to the observations. However, for periods of high M_A, one would assume that the local shear angle at a reconnection site would have to be very high or antiparallel.

The results show that reconnection and subsequent cusp observations can occur during a variety of solar wind conditions. However, the presence of so few cusp examples during overlapping spacecraft orbits implies that the necessary solar wind conditions required for reconnection to occur are not as common at Saturn as at Earth, supporting the conclusion of *Masters et al.* [2012] that reconnection at Saturn is often suppressed to only occur when the magnetic shear of the two magnetic fields is very high (something that cannot be investigated with mSWiM data). This finding also supports the open flux investigation reported by *Badman et al.* [2013]. From a large set of auroral images, the authors found that although Saturn has a similar relative amount of open flux (2–11%) as Earth, the usual percentage of flux that was closed in between observations is much lower (~13%, while at Earth ~40–70%). Assuming that over adequately large timescales, the amount of flux opened is equal to the amount closed, the opening of flux occurs during fewer events or at a lower rate than at Earth. The low number of cusp observations could also, in part, be due to the small spatial size of the cusp at Saturn. If opening of flux occurs at a lower rate, one would expect the spatial extent of the cusp to be lower, and therefore, it would be more likely for Cassini to "miss" it.

8.4. Energetic Electron Events

One hour period bursts of high-energy (~100 keV) electron flux can be seen for some of the magnetospheric observations (adjacent to the cusp). This is most obviously observed in the CAPS-ELS observations for the 3AUG08 event while in the magnetosphere adjacent to the cusp, in the MIMI-LEMMS observations for the 24JUL13 event between 21:00 and 23:00 UT the day before and in the 1FEB07 observation between 20:00 and 23:00 UT. These energetic electrons (LEMMS) are also observed on open field lines in the cusp for the 24SEP08 and 14JUN13 events. During both events periodic pulses are occasionally observed. Energetic electrons, usually associated with magnetosphere, are not expected to be observed on open fields because once the field line is open to the solar wind, these electrons will quickly "drain" out of the magnetosphere. For the 24SEP08 these electrons have pitch angles of both field and antifield aligned, which would probably require energization above and below the observation point, or at the reconnection site, something that we cannot quantify in this paper. Similar observations of energetic electrons have been found to occur on open field lines [*Roussos et al.*, 2015; *Mitchell et al.*, 2016; *Palmaerts et al.*, 2016]. Statistical surveys have shown that these electrons map to the dayside magnetopause [*Roussos et al.*, 2015; *Palmaerts et al.*, 2016]. Their cause is currently not understood; they have been suggested to be related to reconnection processes. Their observations in our events on open field lines in the cusp are also unusual and unexplained. It is interesting to note that the location of our reconnection sites shown in Figure 7 are very similar to the location of a cluster of 1h pulsed electron events on open field lines in the pre noon sector reported by *Roussos et al.* [2015]. Considering this, and that we observe the same pulses near or at the cusp, we agree with previous reports that these pulses may be triggered by magnetic reconnection.

8.5. Conclusions and Further Work

A further eight magnetospheric cusp traversals at Saturn have been presented, which complement previous observations [*Jasinski et al.*, 2014; *Arridge et al.*, 2016]. The observations display considerable variability in their characteristics, such as the ion energy-latitude dispersions, the propagated upstream solar wind conditions,

the plasma composition, and the field-aligned distance to the reconnection site. All the cusp events, except for one, occur where the reconnection site is at the subsolar point. The 8MAR07 cusp event shows evidence for both subsolar and lobe reconnection occurring on the same day. Evidence for bursty or pulsed reconnection was presented similar to the event presented by *Jasinski et al.* [2014] and was observed in the ion energy-latitude dispersions. However, other events also show similarity to the more steady energy-latitude dispersions presented by *Arridge et al.* [2016]. The field-aligned distance to the reconnection site was also found to vary significantly between events. The solar wind propagation shows that the cusp is present for both compressed and expanded magnetospheric conditions, as well as a variety of solar wind Alfvénic Mach numbers.

Strong diamagnetic depressions in the cusp have been widely studied and are often observed at Earth [e.g., *Zhou et al.*, 2001; *Trattner et al.*, 2012] as well as at Mercury [*Winslow et al.*, 2012]. Diamagnetic depressions at Earth have been correlated with highly energetic particles in the cusp [e.g., *Chen et al.*, 1997, 1998; *Nykyri et al.*, 2011a, 2011b]. Such depressions are observed in eight out of the 11 events that have so far been identified at Saturn. Some statistical studies impose criteria on the depth of a diamagnetic depression in order to classify it as such. *Niehof et al.* [2010] use a 20% decrease in magnetic field strength. Using this criterion, some of our observed depressions would not be classified as a diamagnetic depression in our study. The strength of the depression has been suggested to be correlated to the reconnection rate [*Slavin et al.*, 2014], and this could mean that lower reconnection rates (which are expected at Saturn) could thus result in less significant magnetic field depressions. To try and elucidate the physics of the diamagnetic depressions in Saturn's cusp and shed further light on magnetopause reconnection at Saturn, another investigation led by J. M. Jasinski will focus on the diamagnetic depressions.

References

Achilleos, N., C. S. Arridge, C. Bertucci, C. M. Jackman, M. K. Dougherty, K. K. Khurana, and C. T. Russell (2008), Large-scale dynamics of Saturn's magnetopause: Observations by Cassini, *J. Geophys. Res.*, *113*, A11209, doi:10.1029/2008JA013265.

Arridge, C., et al. (2016), Cassini observations of Saturn's southern polar cusp, *J. Geophys. Res. Space Physics*, *121*, 3006–3030, doi:10.1002/2015JA021957.

Badman, S. V., A. Masters, H. Hasegawa, M. Fujimoto, A. Radioti, D. Grodent, N. Sergis, M. K. Dougherty, and A. J. Coates (2013), Bursty magnetic reconnection at Saturn's magnetopause, *Geophys. Res. Lett.*, *40*, 1027–1031, doi:10.1002/grl.50199.

Bunce, E. J., et al. (2008), Origin of Saturn's aurora: Simultaneous observations by Cassini and the Hubble Space Telescope, *J. Geophys. Res.*, *113*, A09209, doi:10.1029/2008JA013257.

Burch, J. L. (1973), Rate of erosion of dayside magnetic flux based on a quantitative study of the dependence of polar cusp latitude on the interplanetary magnetic field, *Radio Sci.*, *8*, 955–961, doi:10.1029/RS008i011p00955.

Burch, J. L., P. H. Reiff, R. A. Heelis, W. B. Hanson, J. D. Winningham, C. Gurgiolo, J. D. Menietti, J. N. Barfield, and R. A. Hoffman (1982), Plasma injection and transport in the mid-altitude polar cusp, *Geophys. Res. Lett.*, *9*, 921–924, doi:10.1029/GL009i009p00921.

Burch, J. L., et al. (1985), IMF B_y-dependent plasma flow and Birkeland currents in the dayside magnetosphere. I—Dynamics Explorer observations, *J. Geophys. Res.*, *90*, 1577–1593, doi:10.1029/JA090iA02p01577.

Burton, R. K., R. L. McPherron, and C. T. Russell (1975), The terrestrial magnetosphere—A half-wave rectifier of the interplanetary electric field, *Science*, *189*, 717, doi:10.1126/science.189.4204.717.

Candidi, M., G. Mastrantonio, S. Orsini, and C.-I. Meng (1989), Evidence of the influence of the interplanetary magnetic field azimuthal component on polar cusp configuration, *J. Geophys. Res.*, *94*, 13,585–13,591, doi:10.1029/JA094iA10p13585.

Cargill, P. J., et al. (2005), Cluster at the magnetospheric cusps, *Space Sci. Rev.*, *118*, 321–366, doi:10.1007/s11214-005-3835-0.

Chapman, S., and V. C. A. Ferraro (1931a), A new theory of magnetic storms, *Terr. Magn. Atmos. Electr.*, *36*, 77–97, doi:10.1029/TE036i002p00077.

Chapman, S., and V. C. A. Ferraro (1931b), A new theory of magnetic storms, *Terr. Magn. Atmos. Electr.*, *36*, 171–186, doi:10.1029/TE036i003p00171.

Chen, J., T. A. Fritz, R. B. Sheldon, H. E. Spence, W. N. Spjeldvik, J. F. Fennell, and S. Livi (1997), A new, temporarily confined population in the polar cap during the August 27, 1996 geomagnetic field distortion period, *Geophys. Res. Lett.*, *24*, 1447–1450, doi:10.1029/97GL01369.

Chen, J., et al. (1998), Cusp energetic particle events: Implications for a major acceleration region of the magnetosphere, *J. Geophys. Res.*, *103*, 69–78, doi:10.1029/97JA02246.

Cui, J., R. V. Yelle, and K. Volk (2008), Distribution and escape of molecular hydrogen in Titan's thermosphere and exosphere, *J. Geophys. Res.*, *113*, E10004, doi:10.1029/2007JE003032.

Desroche, M., F. Bagenal, P. A. Delamere, and N. Erkaev (2013), Conditions at the magnetopause of Saturn and implications for the solar wind interaction, *J. Geophys. Res. Space Physics*, *118*, 3087–3095, doi:10.1002/jgra.50294.

Dougherty, M. K., et al. (2004), The Cassini magnetic field investigation, *Space Sci. Rev.*, *114*, 331–383, doi:10.1007/s11214-004-1432-2.

Dungey, J. W. (1961), Interplanetary magnetic field and the auroral zones, *Phys. Rev. Lett.*, *6*, 47–48, doi:10.1103/PhysRevLett.6.47.

Dunlop, M. W., et al. (2005), Cluster observations of the CUSP: Magnetic structure and dynamics, *Surv. Geophys.*, *26*, 5–55, doi:10.1007/s10712-005-1871-7.

Escoubet, C. P., et al. (2013), Double cusp encounter by Cluster: Double cusp or motion of the cusp?, *Ann. Geophys.*, *31*, 713–723, doi:10.5194/angeo-31-713-2013.

Frank, L. A. (1971), Plasma in the Earth's polar magnetosphere, *J. Geophys. Res.*, *76*, 5202–5219, doi:10.1029/JA076i022p05202.

Fukazawa, K., S.-I. Ogi, T. Ogino, and R. J. Walker (2007), Magnetospheric convection at Saturn as a function of IMF B_Z, *Geophys. Res. Lett.*, *34*, L01105, doi:10.1029/2006GL028373.

Gosling, J. T., M. F. Thomsen, S. J. Bame, T. G. Onsager, and C. T. Russell (1990), The electron edge of the low latitude boundary layer during accelerated flow events, *Geophys. Res. Lett.*, *17*, 1833–1836, doi:10.1029/GL017i011p01833.

Gosling, J. T., M. F. Thomsen, S. J. Bame, R. C. Elphic, and C. T. Russell (1991), Observations of reconnection of interplanetary and lobe magnetic field lines at the high-latitude magnetopause, *J. Geophys. Res.*, *96*, 14,097–14,106, doi:10.1029/91JA01139.

Heikkila, W. J., and J. D. Winningham (1971), Penetration of magnetosheath plasma to low altitudes through the dayside magnetospheric cusps, *J. Geophys. Res.*, *76*, 883–891, doi:10.1029/JA076i004p00883.

Hill, T. W., and P. H. Reiff (1977), Evidence of magnetospheric cusp proton acceleration by magnetic merging at the dayside magnetopause, *J. Geophys. Res.*, *82*, 3623–3628, doi:10.1029/JA082i025p03623.

Jackman, C. M., N. Achilleos, E. J. Bunce, S. W. H. Cowley, M. K. Dougherty, G. H. Jones, S. E. Milan, and E. J. Smith (2004), Interplanetary magnetic field at ∼9 AU during the declining phase of the solar cycle and its implications for Saturn's magnetospheric dynamics, *J. Geophys. Res.*, *109*, A11203, doi:10.1029/2004JA010614.

Jasinski, J. M., et al. (2014), Cusp observation at Saturn's high-latitude magnetosphere by the Cassini spacecraft, *Geophys. Res. Lett.*, *41*, 1382–1388, doi:10.1002/2014GL059319.

Jasinski, J. M., et al. (2016), Flux transfer event observation at Saturn's dayside magnetopause by the Cassini spacecraft, *Geophys. Res. Lett.*, *43*, doi:10.1002/2016GL069260.

Jinks, S. L., et al. (2014), Cassini multi-instrument assessment of Saturn's polar cap boundary, *J. Geophys. Res. Space Physics*, *119*, 8161–8177, doi:10.1002/2014JA020367.

Kanani, S. J., et al. (2010), A new form of Saturn's magnetopause using a dynamic pressure balance model, based on in situ, multi-instrument Cassini measurements,*J. Geophys. Res.*, *115*, A06207, doi:10.1029/2009JA014262.

Khurana, K. K., et al. (2006), A model of Saturn's magnetospheric field based on latest Cassini observations, *Eos Trans. AGU*, *87*(36), Jt. Assem. Suppl., Abstract P44A-01.

Krimigis, S. M., et al. (2004), Magnetosphere Imaging Instrument (MIMI) on the Cassini mission to Saturn/Titan, *Space Sci. Rev.*, *114*, 233–329, doi:10.1007/s11214-004-1410-8.

Lockwood, M., and M. F. Smith (1994), Low and middle altitude cusp particle signatures for general magnetopause reconnection rate variations. 1: Theory, *J. Geophys. Res.*, *99*, 8531–8553, doi:10.1029/93JA03399.

Lockwood, M., T. G. Onsager, C. J. Davis, M. F. Smith, and W. F. Denig (1994), The characteristic of the magnetopause reconnection X-line deduced from low-altitude satellite observations of cusp ions, *Geophys. Res. Lett.*, *21*, 2757–2760, doi:10.1029/94GL02696.

Lockwood, M., S. E. Milan, T. Onsager, C. H. Perry, J. A. Scudder, C. T. Russell, and M. Brittnacher (2001), Cusp ion steps, field-aligned currents and poleward moving auroral forms, *J. Geophys. Res.*, *106*, 29,555–29,570, doi:10.1029/2000JA900175.

Markwardt, C. B. (2009), Non-linear least-squares fitting in IDL with MPFIT, in *Astronomical Data Analysis Software and Systems XVIII, Quebec, Canada, ASP Conf. Ser.*, vol. 411, edited by D. Bohlender, P. Dowler, and D. Durand, pp. 251–254, Astron. Soc. of the Pac., San Francisco, Calif.

Masters, A. (2015), The dayside reconnection voltage applied to Saturn's magnetosphere, *Geophys. Res. Lett.*, *42*, 2577–2585, doi:10.1002/2015GL063361.

Masters, A., et al. (2012), The importance of plasma β conditions for magnetic reconnection at Saturn's magnetopause, *Geophys. Res. Lett.*, *39*, L08103, doi:10.1029/2012GL051372.

Mitchell, D., J. Carbary, E. Bunce, A. Radioti, S. Badman, W. Pryor, G. Hospodarsky, and W. Kurth (2016), Recurrent pulsations in Saturn's high latitude magnetosphere, *Icarus*, *263*, 94–100, doi:10.1016/j.icarus.2014.10.028.

Mozer, F. S., and A. Retinò (2007), Quantitative estimates of magnetic field reconnection properties from electric and magnetic field measurements, *J. Geophys. Res.*, *112*, A10206, doi:10.1029/2007JA012406.

Nichols, J. D., J. T. Clarke, S. W. H. Cowley, J. Duval, A. J. Farmer, J.-C. Gérard, D. Grodent, and S. Wannawichian (2008), Oscillation of Saturn's southern auroral oval, *J. Geophys. Res.*, *113*, A11205, doi:10.1029/2008JA013444.

Niehof, J. T., T. A. Fritz, R. H. W. Friedel, and J. Chen (2010), Size and location of cusp diamagnetic cavities observed by Polar, *J. Geophys. Res.*, *115*, A07201, doi:10.1029/2009JA014827.

Nykyri, K., A. Otto, E. Adamson, E. Dougal, and J. Mumme (2011a), Cluster observations of a cusp diamagnetic cavity: Structure, size, and dynamics, *J. Geophys. Res.*, *116*, A03228, doi:10.1029/2010JA015897.

Nykyri, K., A. Otto, E. Adamson, and A. Tjulin (2011b), On the origin of fluctuations in the cusp diamagnetic cavity, *J. Geophys. Res.*, *116*, A06208, doi:10.1029/2010JA015888.

Ogilvie, K. W., M. A. Coplan, P. Bochsler, and J. Geiss (1989), Solar wind observations with the ion composition instrument aboard the ISEE-3/ICE spacecraft, *Sol. Phys.*, *124*, 167–183, doi:10.1007/BF00146526.

Øieroset, M., P. E. Sandholt, W. F. Denig, and S. W. H. Cowley (1997), Northward interplanetary magnetic field cusp aurora and high-latitude magnetopause reconnection, *J. Geophys. Res.*, *102*, 11,349–11,362, doi:10.1029/97JA00559.

Palmaerts, B., E. Roussos, N. Krupp, W. Kurth, D. Mitchell, and J. Yates (2016), Statistical analysis and multi-instrument overview of the quasi-periodic 1-hour pulsations in Saturn's outer magnetosphere, *Icarus*, *271*, 1–18, doi:10.1016/j.icarus.2016.01.025.

Persoon, A. M., et al. (2009), A diffusive equilibrium model for the plasma density in Saturn's magnetosphere, *J. Geophys. Res.*, *114*, A04211, doi:10.1029/2008JA013912.

Pitout, F., C. P. Escoubet, B. Klecker, and H. Rème (2006), Cluster survey of the mid-altitude cusp: 1. Size, location, and dynamics, *Ann. Geophys.*, *24*, 3011–3026, doi:10.5194/angeo-24-3011-2006.

Pitout, F., C. P. Escoubet, B. Klecker, and I. Dandouras (2009), Cluster survey of the mid-altitude cusp: Part 2: Large-scale morphology, *Ann. Geophys.*, *27*, 1875–1886, doi:10.5194/angeo-27-1875-2009.

Reiff, P. H., J. L. Burch, and T. W. Hill (1977), Solar wind plasma injection at the dayside magnetospheric cusp, *J. Geophys. Res.*, *82*, 479–491, doi:10.1029/JA082i004p00479.

Reisenfeld, D., J. Williams, R. Baragiola, M. Fama, H. Martens, E. Sittler, H. T. Smith, M. Thomsen, and D. Young (2008), The ion composition of Saturn's magnetosphere, in *37th COSPAR Scientific Assembly*, vol. 37, p. 2593, COSPAR Meeting, Montréal, Canada.

Roussos, E., et al. (2015), Quasi-periodic injections of relativistic electrons in Saturn's outer magnetosphere, *Icarus*, *263*, 101–116, doi:10.1016/j.icarus.2015.04.017.

Russell, C. T., C. R. Chappell, M. D. Montgomery, M. Neugebauer, and F. L. Scarf (1971), OGO 5 observations of the polar cusp on November 1, 1968, *J. Geophys. Res.*, *76*, 6743–6764, doi:10.1029/JA076i028p06743.

Shelley, E. G., R. D. Sharp, and R. G. Johnson (1976), He^{++} and H^+ flux measurements in the day side cusp—Estimates of convection electric field, *J. Geophys. Res.*, *81*, 2363–2370, doi:10.1029/JA081i013p02363.

Slavin, J. A., R. E. Holzer, J. R. Spreiter, and S. S. Stahara (1984), Planetary Mach cones—Theory and observation, *J. Geophys. Res.*, *89*, 2708–2714, doi:10.1029/JA089iA05p02708.

Slavin, J. A., et al. (2014), MESSENGER observations of Mercury's dayside magnetosphere under extreme solar wind conditions, *J. Geophys. Res. Space Physics*, *119*, 8087–8116, doi:10.1002/2014JA020319.

Smith, M. F., and M. Lockwood (1996), Earth's magnetospheric cusps, *Rev. Geophys.*, *34*, 233–260, doi:10.1029/96RG00893.

Thomsen, M. F., D. B. Reisenfeld, D. M. Delapp, R. L. Tokar, D. T. Young, F. J. Crary, E. C. Sittler, M. A. McGraw, and J. D. Williams (2010), Survey of ion plasma parameters in Saturn's magnetosphere, *J. Geophys. Res.*, 115, A10220, doi:10.1029/2010JA015267.

Trattner, K. J., S. M. Petrinec, S. A. Fuselier, and R. Friedel (2012), Investigating the relationship between cusp energetic particle events and cusp diamagnetic cavities, *J. Atmos. Sol. Terr. Phys.*, 87, 56–64, doi:10.1016/j.jastp.2011.08.004.

Tseng, W.-L., R. E. Johnson, M. F. Thomsen, T. A. Cassidy, and M. K. Elrod (2011), Neutral H_2 and H_2^+ ions in the Saturnian magnetosphere, *J. Geophys. Res.*, 116, A03209, doi:10.1029/2010JA016145.

Wing, S., P. T. Newell, and J. M. Ruohoniemi (2001), Double cusp: Model prediction and observational verification, *J. Geophys. Res.*, 106(A11), 25,571–25,593, doi:10.1029/2000JA000402.

Winslow, R. M., C. L. Johnson, B. J. Anderson, H. Korth, J. A. Slavin, M. E. Purucker, and S. C. Solomon (2012), Observations of Mercury's northern cusp region with MESSENGER's Magnetometer, *Geophys. Res. Lett.*, 39, L08112, doi:10.1029/2012GL051472.

Young, D. T., et al. (2004), Cassini Plasma Spectrometer investigation, *Space Sci. Rev.*, 114, 1–112, doi:10.1007/s11214-004-1406-4.

Zhou, X. W., C. T. Russell, G. Le, S. A. Fuselier, and J. D. Scudder (2001), Factors controlling the diamagnetic pressure in the polar cusp, *Geophys. Res. Lett.*, 28, 915–918, doi:10.1029/2000GL012306.

Zieger, B., and K. C. Hansen (2008), Statistical validation of a solar wind propagation model from 1 to 10 AU, *J. Geophys. Res.*, 113, A08107, doi:10.1029/2008JA013046.

Zong, Q.-G., et al. (2008), Multiple cusps during an extended northward IMF period with a significant B_y component, *J. Geophys. Res.*, 113, A01210, doi:10.1029/2006JA012188.